Active Site Loop Motion in Triosephosphate Isomerase: T-Jump Relaxation Spectroscopy of Thermal Activation †

ARTICLE *in* BIOCHEMISTRY · APRIL 2003

Impact Factor: 3.02 · DOI: 10.1021/bi026994i · Source: PubMed

5 AUTHORS, INCLUDING:

Ruel Desamero
City University of New York - York College
24 PUBLICATIONS **319** CITATIONS

SEE PROFILE

Ann Mcdermott
Columbia University
100 PUBLICATIONS **4,012** CITATIONS

SEE PROFILE

Active Site Loop Motion in Triosephosphate Isomerase: T-Jump Relaxation Spectroscopy of Thermal Activation†

Ruel Desamero,‡,§ Sharon Rozovsky,‡,|| Nick Zhadin,§ Ann McDermott,*,|| and Robert Callender*,§

Department of Biochemistry, Albert Einstein College of Medicine, Bronx, New York 10461, and Department of Chemistry, Columbia University, New York, New York 10027

Received October 11, 2002; Revised Manuscript Received December 19, 2002

ABSTRACT: As for many enzymes, the enzymatic pathway of triosephosphate isomerase (TIM) includes the partially rate determining motion of an active site loop (loop 6, residues 166−176), which must remain closed during chemistry but must open just before product release. The motion of this loop was monitored using laser induced temperature-jump relaxation spectroscopy at nanosecond to millisecond time resolution. Trp168 in the hinge of the mobile loop served as a fluorophore reporter in a mutant of the yeast enzyme. The opening rate was studied as a function of the concentration of glycerol 3-phosphate, a substrate surrogate. Monoexponential kinetics were observed; assuming a simple two-step ligand release mechanism involving an encounter complex intermediate, the time scales of loop opening and closing were derived. The opening rate of the loop at 25 °C was determined to be 2500 ± 1000 s^{-1}, in remarkable agreement with solution and solid state NMR measurements. The closing rate at the same temperature was 46,700 ± 1800 s^{-1}. The rates were also studied as a function of the sample temperature following the jump. Enthalpies of activation of the loop motion, $\Delta H^{\ddagger}_{close}$ and $\Delta H^{\ddagger}_{open}$, were estimated to be 13.8 and 14.1 kcal/mol, respectively. The enthalpy of dissociation estimated from the kinetic studies is in reasonable agreement with steady-state values. Moreover, the enthalpy was dissected, for the first time, into components associated with ion binding and with protein conformational change. The enthalpy of the release reaction appeared to have a substantial contribution from the dissociation of the ligand from the encounter complex, found to be endothermic at 6 kcal/mol. In contrast, the population ratio of the open to closed loop conformations is found to favor the closed conformation but to be substantially less temperature dependent than the release step. Preliminary data of other ligands show that G3P behavior resembles that of the substrate but differs from 2-phosphoglycolate, a tight binding inhibitor, and phosphate. This study represents one of the first detailed comparisons between NMR and fluorescence based probes of protein motion and results in good agreement between the methods. The data in aggregate support a model in which the rate of the loop opening for TIM is dependent on the ligand and results in opening rates in the presence of the product that are comparable to enzymatic throughput, k_{cat}.

Conformational flexibility is a common feature of enzymes, often used to control chemical reactivity or to deliver a signal from one macromolecule to another. A common element is an active site loop, wherein an open form can facilitate ligand binding and release, and a closed form prepares, controls, and protects the reaction intermediates. In the few examples measured to date, active site loop motion is either rate limiting or closely coordinated with the reaction chemical steps (*1*−*4*).

We have studied the case of triosephosphate isomerase (TIM)[1], where loop 6 controls the catalytic cycle: the interconversion of two glycolytic intermediates, dihydroxyacetone phosphate (DHAP) and D-glyceraldehyde 3-phosphate (GAP) (*4*) (Figure 1A). Internal mobility for TIM was evident as early as 1970 from changes in crystal cell dimensions upon soaking of a ligand (*5*). Kinetic characterization of the free energy profile for the reaction also suggested that substrate release could be rate limiting and is dependent upon the nature of the product (DHAP vs GAP) (*6*). Structural characterization of the enzyme provided direct evidence for the nature of the conformational change in question: loop 6 descends down upon the active site to isolate the reaction from bulk water (*7*−*9*) (Figure 1B). This flexible loop is responsible for shifting the catalytic base, Glu165, by about 2 Å to contact the substrate and centering it in an optimal position between the substrate's relevant carbons (*10*). While many of the crucial catalytic contacts, for example, the polarizing groups His95 and Lys12, and many of the phosphate hydrogen bond partners, such as the NH groups of Gly233 and Ser211, are involved in a preformed substrate pocket and do not shift substantially

† This work was supported by the Institute of General Medicine of the National Institutes of Health Grants GM35183 (R.C.) and GM66388 (A.M.).

* Correspondence should be addressed to the following authors. (R.C.) E-mail: call@aecom.yu.edu. (A.M.) E-mail: aem5@columbia.edu.

‡ These authors contributed equally to this work.

§ Albert Einstein College of Medicine.

|| Columbia University.

[1] Abbreviations: TIM, triosephosphate isomerase; DHAP, dihydroxyacetone phosphate; GAP, D-glyceraldehyde 3-phosphate; G3P, DL-glycerol 3-phosphate; PGA, 2-phosphoglycolate; RMSD, root-mean-square deviation.

10.1021/bi026994i CCC: $25.00
Published on Web 02/19/2003

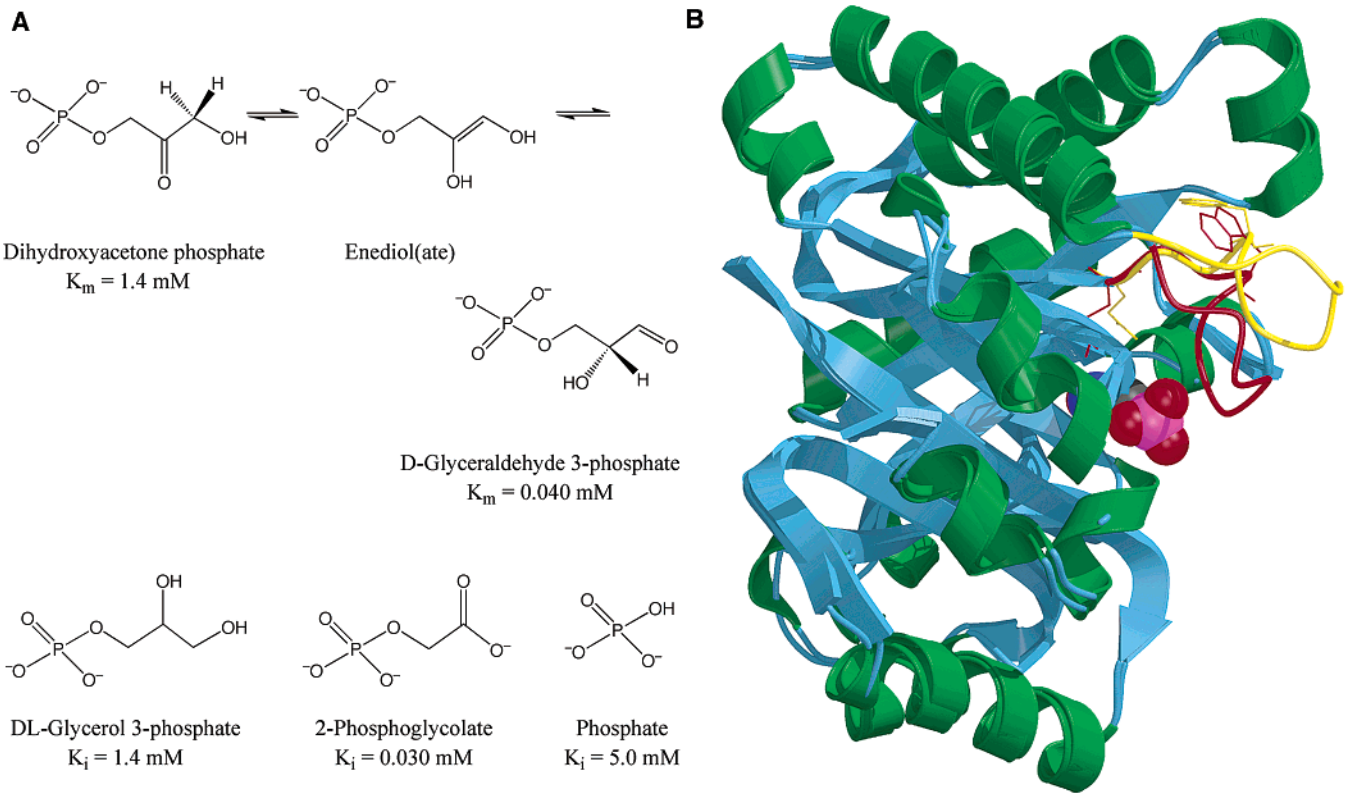

FIGURE 1: (A) Isomerization reaction catalyzed by triosephosphate isomerase. Structure and inhibition constants, K_i, of the ligands studied are listed. (B) An overlay of TIM in the loop open and loop closed (with bound substrate in CPK) conformations. Loop 6 is shown in dark yellow (open) and red (closed), and motion of the indole ring of Trp168 and the active site residue Glu165 are shown as stick diagrams. The active site loop descends down to engulf the substrate and position some of the catalytic residues. The loop's tryptophan rotates by about 50° between the two conformations

upon ligation; others that are attached to loop 6, such as the catalytic base Glu165 and another phosphate ligand, the NH of Gly171, shift into place upon the loop movement. The presence and sequence of the loop is critical for function (*11*), and its sequence is strongly evolutionarily conserved. Kinetic evidence suggests that the loop must close to activate the base and more importantly must remain closed for the duration of the intermediate's lifetime and thereby prevent hydration of the catalytic intermediate and consequent elimination of the phosphate in the enol intermediate to form a toxic sideproduct, methyl glyoxal (*11*, *12*). Thus, the question of the rate of opening in relation to the progress of the chemical reaction becomes of keen interest.

A variety of physical and kinetic studies have been carried out to characterize the loop's structure and dynamics. Site specific mutants in the regions connecting or binding the active site loop have been made with the intention of altering the loop dynamics, and pronounced effects on the reaction rates, kinetic isotope effects, and other functional signatures were seen in some cases (*12*, *13*). Direct measurement of the loop opening rate was recently obtained by solid and solution state NMR (*14*, *15*). A tryptophan on the N-terminal hinge of loop 6 was labeled using either ^{19}F or ^{2}H. NMR line shape analysis, for both solution and solid state samples, demonstrated that the loop opening in the presence of a substrate surrogate, DL-glycerol 3-phosphate (G3P), is on the order of the reaction turnover rate: $8000 \pm 1500\ s^{-1}$ at 30 °C derived from solid state NMR measurements and $5000 \pm 1500\ s^{-1}$ at 30 °C from solution NMR measurements. The rates are clearly much slower at lower temperatures and dependent upon the organic portion of the bound ligand. These studies suggested that the chemical turnover rate and the loop opening rate are of a similar time scale, as required for preventing the phosphate elimination side reaction.

Here, we address the kinetics and thermodynamics of the active site of loop 6 in the presence of various ligands and ligand conditions using temperature-jump relaxation spectroscopy. T-jump relaxation experiments monitor the return to equilibrium of a chemical system following a sudden increase in temperature, here produced by absorption of pulsed laser light tuned to a weak near infrared water band; the adjustment to the new temperature is typically manifested in a change in the concentrations of chemical species. As the system relaxes to this new equilibrium point, a suitable structurally sensitive spectroscopic probe is used to follow the recovery kinetics. For our studies, the fluorescence emission of a strategically placed indole ring of a Trp residue within TIM's loop reports on the time evolution of loop motions over the 20 ns to 1 ms time scale. This protocol is illustrated in Figure 2. The rates of loop-opening and loop-closing and their temperature dependencies are determined by this approach.

Since the loop-opening rate in TIM has recently been determined from NMR relaxation studies, the present study also offers an opportunity for comparison of T-jump relaxation spectroscopy, as combined with fluorescence spectroscopy as a structural reporter, with NMR line shape methods for microsecond motions. Strengths and weaknesses of these two families of methods will sometimes make one more appropriate than the other. NMR spectroscopy offers

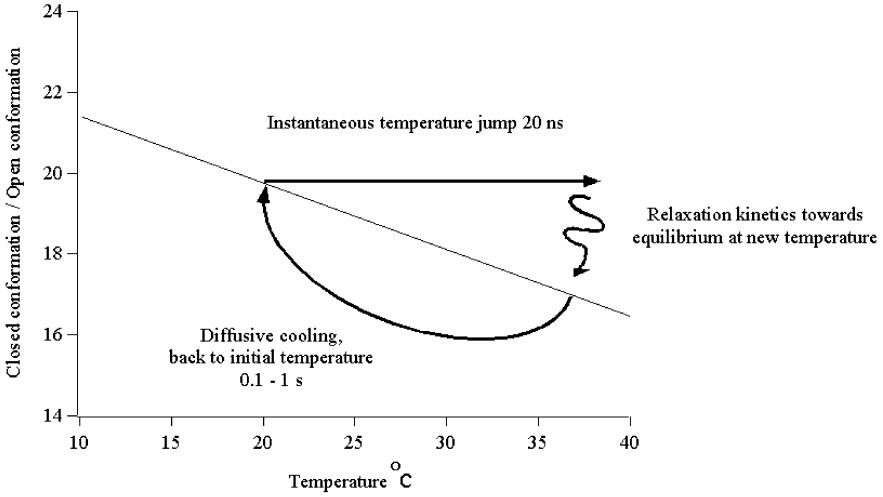

FIGURE 2: Typical response to a temperature jump is shown in cartoon format. Prior to the temperature jump, the system is poised according to the initial temperature with the ratio of bound enzyme and of loop populations fixed accordingly. A rapid temperature change is accomplished bringing the solvent to a higher final temperature in ca. 20 ns in our study. In response to the temperature shift, the TIM−ligand system subsequently relaxes to the new ratio of the open/closed populations defined by the final temperature. In our specific apparatus, roughly 1 ms after the temperature jump, the sample temperature starts drifting back to its initial value because of thermal diffusion. Thus, a kinetic window from 20 ns to 1 ms is afforded for observation of any enthalpic process.

structural signatures in connection with the motion (i.e., can report the spatial extent of the motion or offer direct evidence for the structural substates) (*16*, *17*). On the other hand, the structural origins of fluorescence yield changes are often obscure. Both methods have somewhat limited regimes in which they can work: for NMR, substantial populations for the alternative conformation are usually needed, and changes in the NMR chemical shift are required, whereas for T-jump methods the states must differ in enthalpy, and changes in fluorescence yield for the two states are essential when fluorescence emission is used as a reporter probe of structure. Because of the strong detection sensitivity of fluorescence, optical relaxation spectroscopy can be highly sensitive to motions on a broad range of time scales (as fast as picoseconds, in principle, and as slow as minutes or longer), including rather small population changes, and thus can be expected to reveal conformational events that are too subtle for NMR methods and allow a more thorough dissection of the kinetic properties (*18*, *19*). In the case of the TIM loop motion, however, both NMR and T-jump fluorescence were viable probes of the opening rate. Thus, we were able to test whether quantitative agreement between the two methods is possible and to test whether a cohesive view of TIM loop dynamics can emerge from the combined data.

MATERIALS AND METHODS

All reagents used were purchased from either Sigma-Aldrich Co. (St. Louis, MO) or Fluka (Milwaukee, WI) with the exception of glycerol 3-phosphate dehydrogenase, which was purchased from Boehringer Mannheim Ltd. (Indianapolis, IN).

Sample Preparation. Triosephosphate isomerase mutant of *Saccharomyces cerevisiae* TIM (Trp90Tyr Trp157Phe) was expressed and purified as described before (*14*). The kinetic parameters of the mutant are not distinguishable from those of the wild-type TIM (*13*). Enzymatic activity was determined by the conversion of GAP to DHAP in the presence of TIM and glycerol 3-phosphate dehydrogenase as described by Putman et al. (*20*).

Samples for steady-state fluorescence and T-jump measurements contained TIM in 50 mM Tris-HCl, 50 mM NaCl, pH 7.8, at 25 °C. Steady-state fluorescence studies required 750 μL of a 50 ± 10 μN TIM solution, while a 250 ± 20 μN sample was required for the 175 μL T-jump cell. A limited number of measurements were performed on TIM in absence of a ligand and in the presence of G3P using a triethanolamine buffer (pH = 7.8) to validate that the choice of buffer does not influence the observed kinetics. The observed relaxation rates and response amplitudes were not significantly affected by the change in buffer. Reported temperatures were determined within ±0.5 °C using a thermocouple thermometer.

Fluorescence Spectroscopy. Steady-state fluorescence spectra were measured on a FluoroMax-2 spectrofluorimeter (Instruments S. A. Group, Edison, NJ) with a spectral resolution of 3 nm for both excitation and emission. A sample was held in a 2 × 10 mm quartz cuvette and excited along the short dimension. The wavelength of excitation was 290 nm for all measurements. Contributions to the emission spectra from the Raman scattering bands of the solvent were corrected by subtracting a solvent blank taken under identical condition as the sample. The fluorescence spectra were also corrected for instrument spectral response using an instrument correction factor. The data were collected using DM-3000 software and analyzed with Igor Pro 4.0 (Wavemetrics, Inc., Lake Oswego, OR) software. Errors in determining the fluorescence intensity were around 2%; this incorporates both instrument error and variations in sample preparations.

The dissociation constant, K_d, of G3P from TIM was determined by monitoring changes in the fluorescence intensity, ΔF, as unligated TIM was titrated with increasing amounts of G3P. For a spectrophotometrically monitored titration, ΔF varies with the G3P concentration, [G3P], according to the following equation (*21*):

$$\Delta F = \frac{\Delta F_{max} \times [\text{G3P}]}{\{[\text{G3P}] + K_d\}} \quad (1)$$

where ΔF_{max} is the change in the signal when all the enzyme is in complex, TIM−G3P. K_d was derived at 5, 12, 17, 21, and 30 °C using this expression. The titrations studies are supplied as supplementary data.

T-Jump Measurement. A custom built instrument was used to measure relaxation kinetics, based on the same principles as that described previously (*22*−*24*). Temperature jumps of 10−25 °C were induced by exposing a volume of water to a pulse of infrared light (1.54 μm wavelength, 60−70 mJ energy, 1−2 mm diameter spot on the sample), generated by stimulated Raman shifting the fundamental emission (1.064 μm) of a Quanta-Ray GCR-150 Q-switched Nd:YAG laser (Spectra Physics, Mount View, CA), operating at 1 Hz, in a 1 m long cell filled with methane gas at 450−500 psi. Water absorbed the laser energy and the temperature of the exposed volume increased in approximately 7 ns. The size of the T-jump was calibrated using the change of water IR absorption with temperature, to within 1 °C. Typical T-jump values ranged from 10 to 20 °C. Diffusion of heat out of the interaction volume takes approximately 2 ms. Hence, the apparatus generated a T-jump within 20 ns that remained nearly constant until approximately 1 ms.

To probe changes in the fluorescence intensity of the tryptophan fluorophore, the sample was irradiated by the 290 nm emission line of an Innova 200-25/5 argon ion laser (Coherent, Palo Alto, CA). To avoid photodamage to the sample, the excitation light was modulated using a shutter that allowed 10 ms exposure for every T-jump pulse. Also, the power of the excitation beam was attenuated by neutral density filters; typical intensity was 15−20 mW. The incident excitation beam is focused onto a 0.5 mm diameter spot on the sample, in the center of the beam path of the 1.54 μm pulse. Tryptophan fluorescence emission, detected at 50° to the excitation beam, was passed through a narrow band filter (340 ± 12 nm) and was monitored using a R4220P photomultiplier tube (Hamamatsu, Bridgewater, NJ). Two oscilloscopes (TDS 754A and TDS 420A, Tektronix, Inc., Beaverton, OR) averaged and digitized all signal generated from 1000 to 2000 heating pulses. To null out a reproducible dc offset voltage arising from the amplifier (2−3% of total signal) and early time pulse-like feature produced by the Nd:YAG laser circuitry via a ground loop (2−3%), a background signal obtained without fluorescence excitation was measured separately and subtracted from the kinetic data. A lab written program from LabVIEW software (National Instruments, Austin, Texas) was used for instrument control and data collection. Data were normalized to the average fluorescence intensity taken before the T-jump. Curve fitting was done with Igor Pro 4.0 (Wavemetrics, Inc., Lake Oswego, OR) software. The uncertainties in the reported values of relaxation rates were determined from the scatter in values from 4 to 5 replicate runs and were approximately ±10% of the measured relaxation rate. Errors in the response amplitudes were analyzed in the same manner and were estimated to be ±20−25%.

RESULTS

Experimental Design. To study loop dynamics, we used a mutant of *S. cerevisiae* TIM (Trp90Tyr Trp157Phe) where a single remaining tryptophan, Trp168, located at the N-terminal hinge of loop 6 served as a spectroscopic probe (Figure 1B). Tryptophan residues are valuable fluorescence probes since the indole ring is very sensitive to its environment (*18*, *25*−*27*). In TIM, the tryptophan's indole ring is not in contact with the bound ligand and therefore is expected to be a reporter of the loop closure and not of the ligand's nearby presence. Stacking of the indole ring, solvation, and hydrogen bond partners differ for the two loop conformations, and therefore the fluorescence yield would be expected to differ. Prior studies (*12*, *13*) on the steady-state fluorescence of this mutant confirmed that the ligated, closed state is quenched relative to the open, unligated state. In both the fluorescence and our previously reported NMR experiments, the system was poised at conditions (pH, ionic strength) that maximize enzymatic activity (*28*, *29*).

Loop dynamics in the presence of the substrate or product is of the most mechanistic significance, but we were obliged to study the motion of the TIM loop using a substrate surrogate (Figure 1A), rather than the authentic substrate, since there is a limited temperature range in which the substrate is stable for long data acquisitions (*30*). DL-glycerol 3-phosphate (G3P) is a substrate mimic, whose binding affinity is similar to that of DHAP; K_i is 1.4 ± 0.3 mM while K_m is 1.4 ± 0.1 mM (*31*). Moreover, a limited set of experiments using substrate as ligand in the T-jump studies yielded similar relaxation rates as found for G3P (see below). Two additional ligands were used to demonstrate that the kinetics do depend on the selection of active site ligand. 2-phosphoglycolate (PGA), considered a mimic of the transition state (*32*), has a K_i of 30 ± 6 μM (*28*). The third ligand studied, inorganic phosphate, contributes significantly to the substrate's binding energy (*33*) and has a K_i of 5.0 ± 0.1 mM (*28*). This simple inhibitor induces the closed loop conformation (*34*) and thus could offer a possible view to binding events as distinct from chemical events. A complete characterization of the G3P ligand was conducted, while the studies of the other ligands serve as preliminary controls.

Steady-State Fluorescence. Steady-state fluorescence of the active site loop's tryptophan was measured as a function of temperature and ligand selection (Figure 3). The fluorescence intensity of the tryptophan in the unligated enzyme was quenched by 25% upon heating the sample from 0 to 35 °C. This is smaller than the observed 60% quenching of fluorescence for tryptophan in solution by itself. The fluorescence intensity was modulated upon addition of ligands (see inset in Figure 3); a 25% decrease in fluorescence intensity as compared to unligated TIM was observed in the presence of PGA, while for G3P the intensity decreased by about 40%. With inorganic phosphate, the fluorescence intensity was quenched by 10%. The wavelength of maximal fluorescence emission was essentially unaffected by the presence of the ligand (λ_{max} = 325 ± 2 nm). To further investigate the possible temperature dependence of loop motion, the dissociation constant (K_d) for TIM with G3P was measured and found to decrease with temperature from (13.2 ± 1.6) × 10^{-4} M at 29.6 °C to (3.0 ± 0.4) × 10^{-4} M at 5.1 °C (Table 1). A van't Hoff analysis of these numbers shows that the overall release of G3P from TIM is endothermic at 10 ± 1 kcal/mol.

T-Jump Relaxation. The simplest kinetic scheme anticipated for the loop opening reaction has two steps:

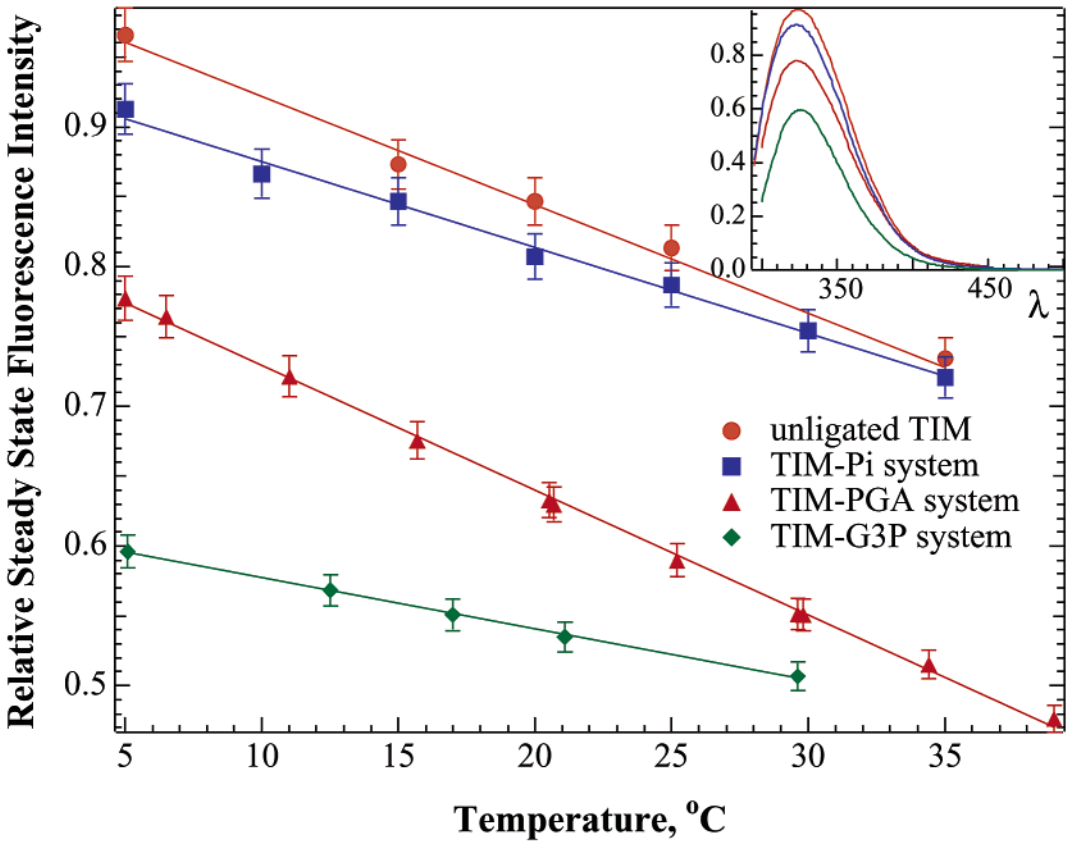

FIGURE 3: Steady-state fluorescence intensity of Trp168 in TIM is affected by temperature modulation and ligands presence; fluorescence spectra in the presence of ligands are shown in the inset. All reported fluorescence intensities are normalized relative to the fluorescence intensity of the unligated TIM measured at 0 °C and at 50 μM TIM. The concentrations of the ligands in each case were as follows: 10 mM G3P, 1.5 mM PGA, and 50 mM phosphate.

Table 1: Temperature Dependence of the Dissociation Constants, K_d, for TIM Bound with G3P

T (°C)	K_d (M)[a]
5.1	$(3.0 \pm 0.4) \times 10^{-4}$
12.5	$(5.3 \pm 0.6) \times 10^{-4}$
17.0	$(6.8 \pm 0.7) \times 10^{-4}$
21.1	$(8.8 \pm 1.2) \times 10^{-4}$
29.6	$(13.2 \pm 1.6) \times 10^{-4}$

[a] K_d values were determined from a fit to the plot of the change in fluorescence intensity against the ligand concentration. Errors reflect the RMSD of the fit.

Scheme 1

$$\text{TIM} + \text{ligand} \underset{k_{off}}{\overset{k_{on}}{\rightleftharpoons}} \text{TIM}^{open}/\text{ligand} \underset{k_{open}}{\overset{k_{close}}{\rightleftharpoons}} \text{TIM}^{closed}/\text{ligand}$$

The equilibrium between the open and the closed forms of the loop and the bound and free states are expected to shift according to temperature. The shift is expected to correspond overall to ligand release (i.e., from right to left in Scheme 1) in a pathway with a slow conformation change followed by a rapid release for each molecule. Prior biochemical evidence supports a low affinity for ligands with an open loop conformation (*11*). The obligate encounter complex intermediate, TIM^{open}/ligand, is expected to be sparsely populated based on these data and others. In what follows below, we use the convention that $\Delta H_{release}$ and $\Delta H_{loop\ motion}$ refer to the enthalpic change because of ligand release from the encounter complex and the loop opening steps given in Scheme 1, respectively.

Figure 4 shows the kinetic response to a 17 °C T-jump of the emission of the Trp168 indole ring as stimulated at 290 nm and measured at 340 nm; the behavior of the TIM in several distinct complexes is contrasted, and these differences will be highlighted in the discussion below. Following the laser induced T-jump, the subsequent thermalization of the excited water molecules results in a prompt temperature increase (subnanosecond) (*35*, *36*). The magnitude of the temperature change and the initial temperatures were varied; a typical T-jump value varies from 10 to 20 °C, and initial temperature was varied from 2 to 40 °C. An abrupt unresolved drop of apparent fluorescence intensity generally ensues upon heating followed by a resolved nanosecond rise in intensity. These relatively rapid kinetic components include the response time of the instrument (4 ns), the pulse width of the heating beam (7 ns), fluorescence lifetime of a few nanoseconds, as well as a protein-dependent phase of unknown origin (20−50 ns) (*37*). These nanosecond phases were not analyzed in this study. A slower instrumentally determined kinetic transient, with a time constant of 1.5 ± 0.5 ms, was attributed to cooling of the irradiated volume by thermal diffusion and was also neglected in this study. Thus, the kinetic window over which we follow loop motions covers over 5 orders of magnitude in time scale, roughly from 0.1 μs to 1 ms.

For unligated TIM (Figure 4) this temporal region is flat, much like the kinetic profile for tryptophan in solution by itself (data not shown). Structural data suggest that the unligated enzyme is mostly in the open loop conformation,

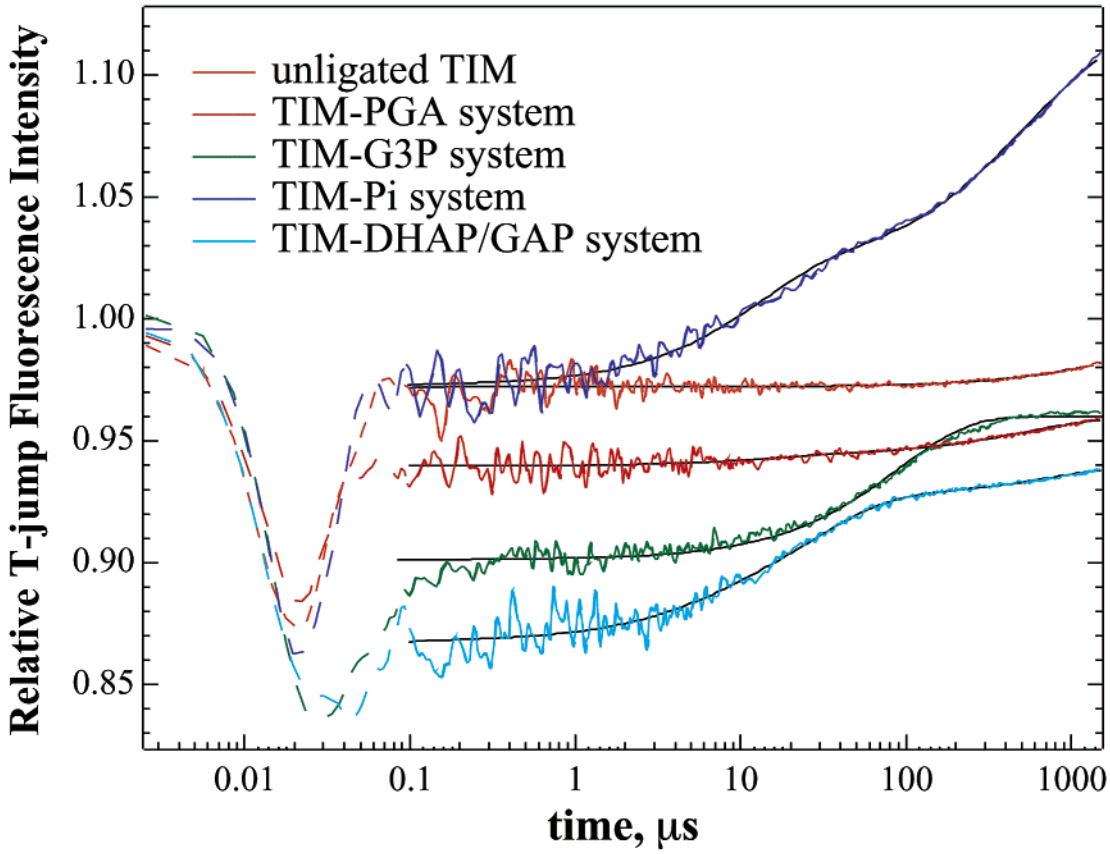

FIGURE 4: Kinetic response of the fluorescence signal is shown for the emission of the tryptophan indole ring as excited at 290 nm and measured at 340 nm, subjected to approximately a 17 °C T-jump. Data from samples of unligated TIM and of TIM in the presence of G3P, GAP, PGA, or phosphate are plotted together to show that the observed effect is strongly sensitive to the selection of the ligand. In all T-jump studies, the total TIM concentration is 250 μM. The ligand concentrations used were near or above saturating concentrations: 5 mM G3P, 5 mM GAP, 1.5 mM PGA, and 50 mM phosphate. For the unligated TIM, kinetic profile in this region is flat. The relaxation kinetics for TIM ligated with 5 mM G3P has a profile in the region between 0.1 μs and 1 ms that could be fit using a single exponential transient. TIM ligated with 5 mM GAP, which rapidly equilibrates to a GAP/DHAP mixture, appeared to exhibit a very similar kinetic profile except for a slightly shorter relaxation time. The kinetic profile of TIM ligated with 1.5 mM PGA has kinetic transients of the order of the noise under these conditions. More complex relaxation kinetics is observed for the TIM ligated with 50 mM phosphate. The region of the kinetic plots over which we follow loop motion, from 0.1 μs to 1 ms, is represented in solid lines. The temperature jumps in each case were as follows: TIM, 2.8−17.7 °C; TIM−PGA, 6.4−19.7 °C; TIM−G3P, 3.0−20.0 °C; TIM−Pi, 8.0−22.5 °C; and TIM−DHAP/GAP, 3.0−19.3 °C.

but prior NMR relaxation data indicate facile small amplitude motions on the microsecond to nanosecond time scale (*38*). The lack of appreciable kinetic components in the fluorescence data indicate that these motions are either faster than 50 ns or involve states of comparable enthalpy or similar fluorescence emission yields.

The T-jump response in the presence of ligands depended dramatically upon the choice of the ligand. For G3P and GAP, a transient of large amplitude could be fit to a single exponential. This kinetic phase is assumed to be associated with the opening of the loop and is analyzed in detail for the case of G3P (vide infra). Significantly, measurements in the presence of the substrate GAP (which rapidly equilibrates to a GAP/DHAP mixture on the time scale of the T-jump study) at low temperature reveal a similar relaxation phenomena, in amplitude and rates, as that observed for the substrate surrogate G3P. To verify that this relaxation process is related to the loop's structural changes, we have examined the effect of choice of ligand on the relaxation phenomena.

In the presence of various concentrations of a mimic of the transition state, PGA (*32*), which has a K_i of 30 ± 6 μM (*28*), no kinetic phase was observed on the microsecond time scale. This process appears to be largely out of our time window (slower), or we are insensitive to it under the conditions of the experiment shown in Figure 4 (i.e., saturating amounts of ligand or a small pH change induced by the T-jump). It is clear that at 1 ms the TIM−PGA system has not yet reached equilibrium at the new temperature. In an attempt to maximize observation of PGA release, the diameter of the incident laser heating beam was widened, which had the effect of increasing the cooling time within the irradiated volume from 2 ms to ca. 31 ms. Under conditions where a substantial fraction of TIM binding sites are unoccupied (total [PGA] = 100 μM, total [TIM] = 250 μM), a situation expected to yield higher signal amplitudes, a temperature-dependent transient of 5−10 ms was observed (data not shown). Indeed, a tighter inhibitor would be expected to involve higher energy barriers for the motion and slower rates, and this result is also comparable to our prior NMR studies on the TIM−PGA complex, where loop motions on the microsecond time scale were not detected.

The kinetic behavior is dramatically different when phosphate is used, a loosely binding inhibitor with a K_i of 5.0 ± 0.1 mM (*28*). The phosphate moiety contributes significantly to the substrate's binding energy (*33*) and induces the closed loop conformation (*34*) but is known to

have substantial liberty in its placement relative to the phosphate's binding amides in the active site and therefore to have a somewhat lesser control over the active site loop (*39*). Complex multi-rate relaxation kinetics were observed for the enzyme in the presence of phosphate. This complex kinetic behavior is consonant with sloppy fit of this minimal ligand in the active site. In summary, it appears that relaxation phenomena are sensitive to the presence and choice of ligand in a manner suggesting the expected behavior of a loop shielding reaction intermediates.

A comparison of the transients in Figure 4 to the steady-state emission data of Figure 3 shows that the observed transient emission has not reached an equilibrium value by 1 ms, the end of the useful range of our T-jump spectrometer. Thus, there must be slower kinetic step or steps. In experiments comparing the response kinetics of temperature versus the fluorescence of protein solutions within the sample cuvette holders of our fluorescence spectrometer, this slow step(s) is shown to be reversible and to relax within 30 s. Thermodynamic signatures show that the kinetic phase in our time window corresponds to the binding and release of ligand (vide infra). Therefore, we made the assumption that this additional kinetic phase does not affect our conclusions regarding analysis of the observed faster transients.

TIM−G3P System. For the TIM−G3P system, the observed relaxation kinetics vary with both the final temperature of the T-jump and the ligand concentration (Figures 4−6). For each condition, the kinetic data were well-simulated using a single-exponential profile. On the basis of the data presented in Figure 4, the rate constant and the amplitude of the relaxation kinetic profile decrease as the concentration increases. At higher temperatures, the rate constant increases (Figure 6).

Kinetic Model. The observed rate for TIM−G3P, k_{obs}, varied in a smooth fashion when the concentration of free ligand and protein was varied. These data are presented in Figure 5, and a fit is presented in Figure 6 based on the kinetic model of Scheme 1. The observed relaxation time is not described by a simple bimolecular reaction of substrate binding to protein; for such a process the observed rate would scale linearly with concentration, whereas for our data saturation behavior is observed. The saturated enzyme also exhibits a concentration and temperature independent kinetic transient. Hence, our kinetic model also includes both a bimolecular and a monomolecular step. A protein−ligand encounter complex, with TIM in the loop open conformation, is formed rapidly through bimolecular collision. This phase is apparently formed too quickly to be observed by our instrument. After the formation of an encounter complex, the protein complex undergoes loop closure in a slow step, probed in these experiments. The rate of the second conformational step is influenced by the concentrations of free protein and ligand through the concentration of TIM^{open}−G3P. The dependence of the loop closure step on various parameters can be derived following a linearization of the kinetic equations of the process in Scheme 1 provided that the fast limit approximation, $k_{on}([TIM] + [G3P]) + k_{off} \gg k_{open}, k_{closed}$, is valid (*19*, *21*, *40*):

$$k_{obs} = \frac{k_{close}}{1 + k_{off}/(k_{on}\{[TIM] + [G3P]\})} + k_{open} \quad (2)$$

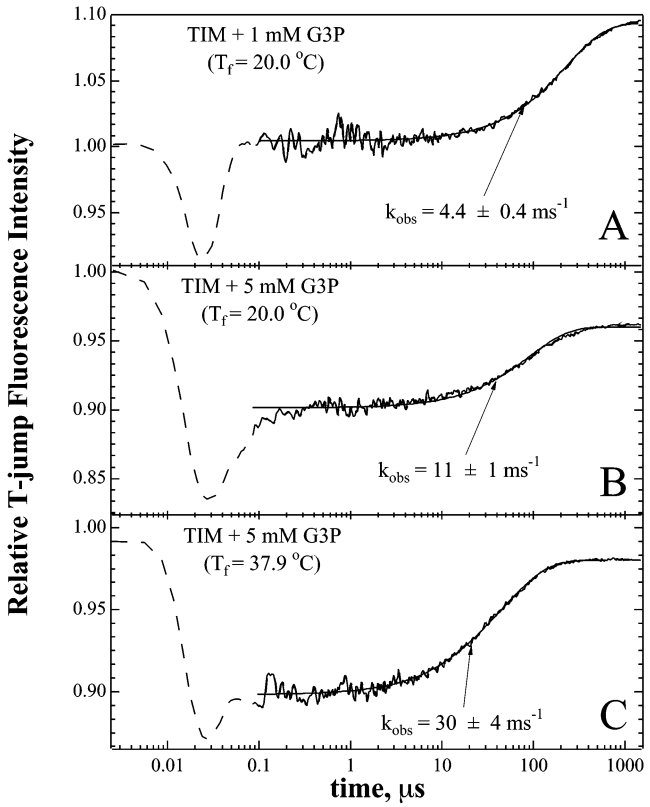

FIGURE 5: Relaxation kinetics of the TIM−G3P complex are shown for a variety of sample conditions, along with a simulation using single exponentials. At 1 mM G3P (panel A), the single-exponential fit to the 0.1 μs to 1 ms region of the kinetic profile yielded a relaxation rate of 4.4 ± 0.4 ms^{-1}. A similar fit to the kinetic profile of TIM ligated with 5 mM G3P resulted in a faster relaxation rate of 11 ± 1 ms^{-1} (panel B). Increasing the final jump temperature (T_f) results in a faster relaxation rate; at a T_f of 20.0 °C the relaxation rate is 11 ± 1 ms^{-1} (panel B), while at 37.9 °C a relaxation rate of 30 ± 4 ms^{-1} is obtained (panel C). Uncertainties in the reported values of the relaxation rate reflect the scatter in values from replicate runs and are much larger than fitting uncertainties from a single run. The region of the kinetic plots over which we follow loop motion, from 0.1 μs to 1 ms, is represented in solid lines. The initial temperatures of the temperature jumps in each case were as follows: (A) 10.0 °C; (B) 3.0 °C; and (C) 20.6 °C.

We used this functional form to fit the results of Figure 6 (solid curves), and the values of k_{open}, k_{closed}, and k_{on}/k_{off} are obtained (Table 2). It should be noted that the monomolecular step of Scheme 1, the rate of which is represented in eq 2, is strictly linear (no high order corrections terms) so that a linear response is expected despite the large T-jumps of this study. On the other hand, in principle the bimolecular step of the kinetic model in Scheme 1 leads to nonlinear kinetic terms. The relative error resulting from neglecting this term is given by $k_{on}\Delta[TIM]/\{(k_{on}([TIM] + [G3P]) + k_{off})\} < k_{on}\Delta[TIM]/k_{off}$ (eq 5.2 of ref *19*), where $\Delta[TIM]$ is the amount of free TIM brought about by the T-jump. Given that k_{on}/k_{off} is no larger than 100 M^{-1}, and $\Delta[TIM]$ is at most 250 μM (the total concentration used in the experiments), the relative error is expected to be less than 1%.

From the kinetically extracted values of k_{open}, k_{closed}, and k_{on}/k_{off}, one can also obtain an estimate of the equilibrium K_d as follows:

$$K_d = (k_{off}/k_{on})(k_{open}/k_{close}) \quad (3)$$

Remarkably, the K_d calculated here agrees with what was

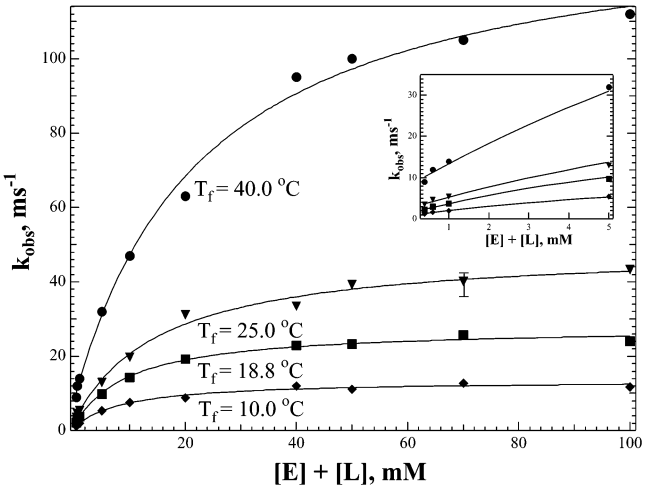

FIGURE 6: Rate of signal relaxation, k_{obs} (see Figure 5), in response to a T-jump for the G3P ligated TIM system is plotted for various final jump temperatures and ligand concentrations. A fit to the plot of k_{obs} vs the sum of the free ligand and free enzyme concentration to eq 2 yields the values of k_{open}, k_{closed}, and k_{on}/k_{off} (see Table 2). The total TIM concentration is 250 μM in all cases. For high ligand concentrations, the dependence on ligand concentration is pseudo-first order. At lower ligand concentrations, the amount of free species at the final temperature were calculated using the temperature-dependent dissociation constants (Table 1). For clarity, a lone *y* axis error bar was used to represent the error in the values of k_{obs}, which ranged within 10−12%. The insert amplifies the *x* axis to better show the rates at low G3P concentrations.

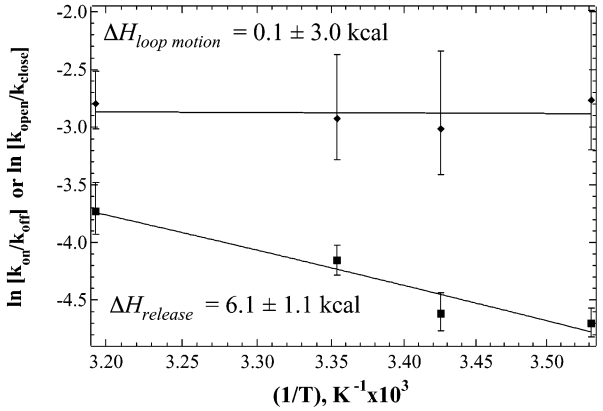

FIGURE 7: van't Hoff plot based on the values of the elementary equilibrium constants k_{on}/k_{off} and k_{open}/k_{close} (Table 2). A linear fit to the plot yields the values for the enthalpic change for loop motion, $\Delta H_{loop\ motion}$, and for ligand release, $\Delta H_{release}$, which were determined to be 0.1 ± 3.0 and 6.1 ± 1.1 kcal, respectively. The *y* axis error bars reflect the propagated errors in the values of ln(k_{on}/k_{off}) and ln(k_{open}/k_{close}). Uncertainties in the value of the determined ΔH values were first approximated as the RMSD of the fit. For $\Delta H_{release}$ this approximation was deemed appropriate because it was consistent with the error bars on the value of ln(k_{on}/k_{off}). For $\Delta H_{loop\ motion}$, however, because of the large error in the values of ln(k_{open}/k_{close}), the RMSD of the fit underestimates the true error of the measurement. To estimate the error of $\Delta H_{loop\ motion}$, we generated two lines that bisect halfway through the lower and upper side of the error bars of the first and last points of the plot: one of the lines slopes upward and another downward. The slopes of these two lines are the quoted error in $\Delta H_{loop\ motion}$.

previously determined by Knowles and Albery (*6*). The K_d values obtained using the kinetic data are also consistent with what was determined using steady-state fluorescence (Table 1). This suggests that the kinetics probed in this study do encapsulate the majority of the binding and release phenomenon and that any slower or faster steps are minor contributions to the thermodynamics of the process.

The kinetic transients can be studied as a function of temperature to derive, separately, the enthalpy changes in ligand release and the enthalpy in loop opening. A van't Hoff plot of k_{on}/k_{off} yields an enthalpy for ligand release the encounter complex, $\Delta H_{release} = 6.1 \pm 1.1$ kcal/mol (Figure 7). Thus, this term favors binding of the ligand to the open loop structure but is only responsible for 60% of the enthalpy in the steady-state value. Correspondingly, the equilibrium constant derived from k_{open}/k_{closed} clearly favors the closed state, but the temperature dependence in these rates was small and was not sufficiently precise to decompose the free energy change further: $\Delta H_{loop\ motion} = 0.1 \pm 3.0$ kcal/mol (favoring the closed species). (The analysis of the response amplitudes given below is in agreement with this range but suggests that ΔH can only favor the closed loop conformation, see below.) The sum of these values ($\Delta H = 6.1 \pm 4.0$ kcal/mol) are of the same sign and order of magnitude as the total enthalpy of release of ligand obtained from steady-state measurements (10 ± 1 kcal/mol, for steady state, see above). The binding energy derived from steady-state measurements is also in good agreement with isothermal titration measurements (data not shown).

Activation parameters for the loop motion can be derived from these rates but have not been derived for the binding and release steps. A van't Hoff plot (Figure 8) based on our experimental values for k_{open} yielded a value of 14.1 ± 2.5 kcal/mol for the activation enthalpy associated with loop opening, $\Delta H^{\ddagger}_{open}$. Correspondingly, the activation enthalpy for loop closing, $\Delta H^{\ddagger}_{close}$, was determined to be 13.8 ± 0.4 kcal/mol. These values are consistent with the pronounced temperature dependence in the rates seen previously by NMR studies (*14*, *15*).

Relaxation Response Amplitude. The variation in the amplitude of the observed relaxation response for the TIM−G3P system is given in Figure 9. The response amplitude can be accounted for using the kinetic model of Scheme 1. The amplitude peaks at a value near K_d and exhibits a plateau at saturating concentrations of G3P. At low concentrations the system is dominated by bimolecular behavior, while at

Table 2: Rate Constants for the Loop Dynamic in TIM at Different Final Temperatures after T-Jump

T_f (°C)	k_{open} (s^{-1})[a]	k_{closed} (s^{-1})[a]	k_{off}/k_{on} (M)[a]	K_d (M)[b]
10.0	800 ± 400	12700 ± 600	0.0091 ± 0.0020	(6 ± 3) × 10^{-4}
18.8	1300 ± 600	26500 ± 700	0.0099 ± 0.0013	(5 ± 2) × 10^{-4}
25.0	2500 ± 1000	46700 ± 1800	0.0157 ± 0.0026	(8 ± 4) × 10^{-4}
40.0	8000 ± 1900	(1.31 ± 0.05) × 10^5	0.024 ± 0.003	(15 ± 4) × 10^{-4}

[a] The values of k_{open}, k_{closed}, and k_{off}/k_{on} are deduced from the fit of the data presented in Figure 5 to eq 2. Their uncertainties are the RMSD of the fit. [b] The value of K_d is calculated from the values of k_{open}, k_{closed}, and k_{off}/k_{on} according to eq 3. The uncertainty in the K_d is propagated from the uncertainties of k_{open}, k_{closed}, and k_{off}/k_{on}.

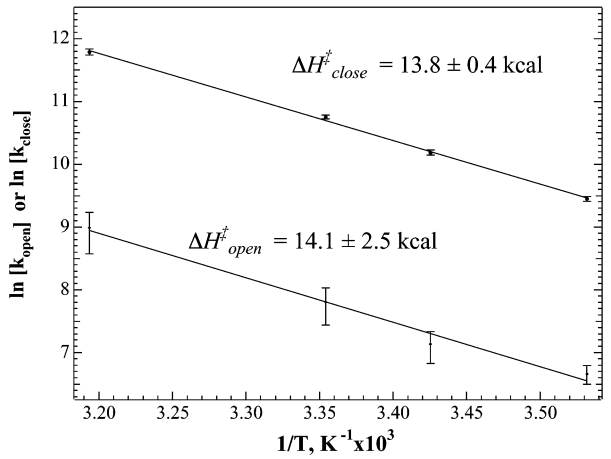

FIGURE 8: van't Hoff plot based on the values of the rate constants k_{open} and k_{close} (Table 2) is used to extract activation parameters. A linear fit to the plot gives the values for the activation enthalpic change for loop opening, $\Delta H^{\ddagger}_{open}$, and loop closing, $\Delta H^{\ddagger}_{close}$, which were determined to be 13.8 ± 0.4 and 14.1 ± 2.5 kcal, respectively. The error bars on the *y* axis reflect the propagated error in the values of ln(k_{open}) and ln(k_{close}). Uncertainties in the value of the determined ΔH values were first approximated as the RMSD of the fit. For $\Delta H^{\ddagger}_{close}$, this approximation was deemed appropriate because it was consistent with the error bars on the value of ln(k_{close}). For $\Delta H^{\ddagger}_{open}$, however, because of the large error in the values of ln(k_{open}), the RMSD of the fit underestimates the true error of the measurement. The procedure outlined in Figure 7 was used to estimate the error in $\Delta H^{\ddagger}_{open}$.

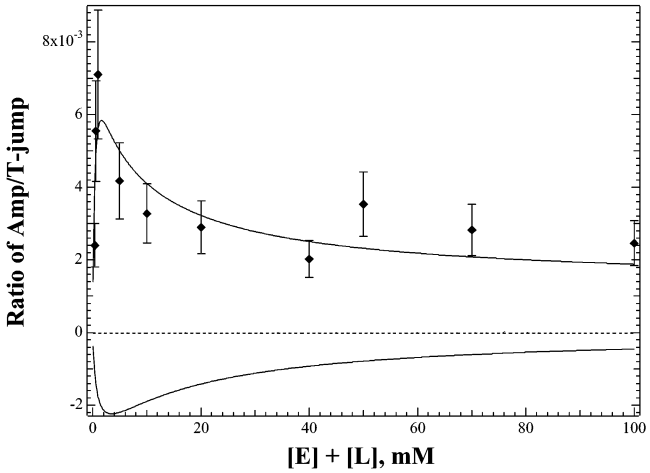

FIGURE 9: Amplitude of the observed loop motion response to the T-jump divided by the size of the T-jump (◆). The *y* axis errors bars, estimated as ±25%, represent the scatter in values from replicate runs and are much larger than the RMSD fit to a single run. The solid lines are theoretical predictions of the amplitude for the loop motion (upper) and ligand release (lower) steps, using parameters described in the text.

high inhibitor concentrations the T-jump results in insignificant G3P release, and a unimolecular interconversion of the ligated open loop species (encounter complex) might dominate the behavior. These phenomena can be quantitatively modeled. Several parameters govern the intensity of these relaxation responses: the enthalpies and equilibrium constants of the reactions and the fluorescence emission coefficients of the indole ring in TIM (ϵ_{TIM}), TIM^{open}−G3P (ϵ_o), and TIM^{closed}−G3P (ϵ_c) (see, for example, eq 3.25; ref *41*). Initial guesses for the equilibrium constants of the reactions and the enthalpies can be derived from the fitting of our data based upon eq 3. The data in Figure 9 are most easily simulated with an assumed small positive $\Delta H_{loop\ motion}$ and larger emission intensities for the encounter complex than for the closed ligated or the open unligated state. The fit to the data, using the functional form of the intensity given by eq 3.5 in ref *41*, assumes values of $\Delta H_{release}$ = 6.0 kcal/mol, a ratio of $\epsilon_{TIM}/\epsilon_c$ = 1.4 (derived from Figure 3), and $\Delta H_{loop\ motion}$ at +2.0 kcal/mol (favoring the closed state), yields a ratio 2.4 for ϵ_o/ϵ_c. These values are not uniquely derived from these data sets. Using $\Delta H_{loop\ motion}$ = +1.0 kcal/mol and ϵ_o/ϵ_c = 2.7 results in an equally good fit. In principle, the positive direction of the observed relaxation response can also be explained by an enthalpy favoring the TIM^{open}−G3P species and ϵ_o/ϵ_c < 1. However, the results are in disagreement with the range of enthalpy set by the kinetics analysis above. For example, the smallest $\Delta H_{loop\ motion}$ is given by setting ϵ_o = 0, which yields $\Delta H_{loop\ motion}$ = −7.0 kcal/mol. At this time, we have no specific structural explanation for the proposed higher emission yield for the encounter complex, although ratios of this magnitude for indole rings in various protein environments are common. Also, it is to be noted that if both enthalpy of the Gibbs free energy term and K_{eq} favor the TIM^{closed}−G3P species over TIM^{open}−G3P, then the entropy term between the two conformations varies within the constraints of our errors but is small.

The bottom trace in Figure 9 shows the calculated intensity of the release step, relative to the loop opening step, given the parameters derived above. The negative amplitude results from the fact that the T-jump induces ligand release, and the indole ring fluorescent efficiency of unligated TIM is substantially smaller than TIM^{open}−G3P.

Although a two step model was assumed, only one kinetic phase was observed. A likely explanation for the observation of a single kinetic phase, dominated by loop motion kinetics, is that the first bimolecular binding step was too fast for our instrument. On the basis of the amplitude calculations above, our experimental sensitivity would have been sufficient to observe the first step provided it had fallen within our experimental time window of 0.1 μs to 1 ms. If the relaxation rate of the release step is given by $k^{obs}_{release} = k_{on}([TIM] + [G3P]) + k_{off}$, if $k_{on} \geq 10^9$ M^{-1} s^{-1}, and considering $k_{off}/k_{on} \approx 0.01$ M (Table 2), then $k^{obs}_{release}$ is expected to be $\geq 10^7$ s^{-1} and unobserved in the present study.

DISCUSSION

The studies described herein allow us to extract the kinetics of loop motions from the 0.1 μs to the 1 ms time scale for the TIM−ligand system. The simple exponential rate constants observed in these studies reflect loop motion and ligand binding as validated in a variety of ways. The smooth dependence of the rates and amplitudes on substrate concentration and temperature allowed us to extract steady-state parameters such as binding constants of the ligand and enthalpies of binding and kinetic parameters, such as the rates and activation enthalpies describing the loop opening, using the minimal kinetic model in Scheme 1. These parameters values are in reasonable agreement with the steady-state values derived from enzyme kinetics and from steady-state fluorescence methods. The qualitative effects of the selection of the ligand are also strong evidence that the process we detect reflects both loop opening and ligand release. With all of this supportive evidence, it is clear that the kinetic

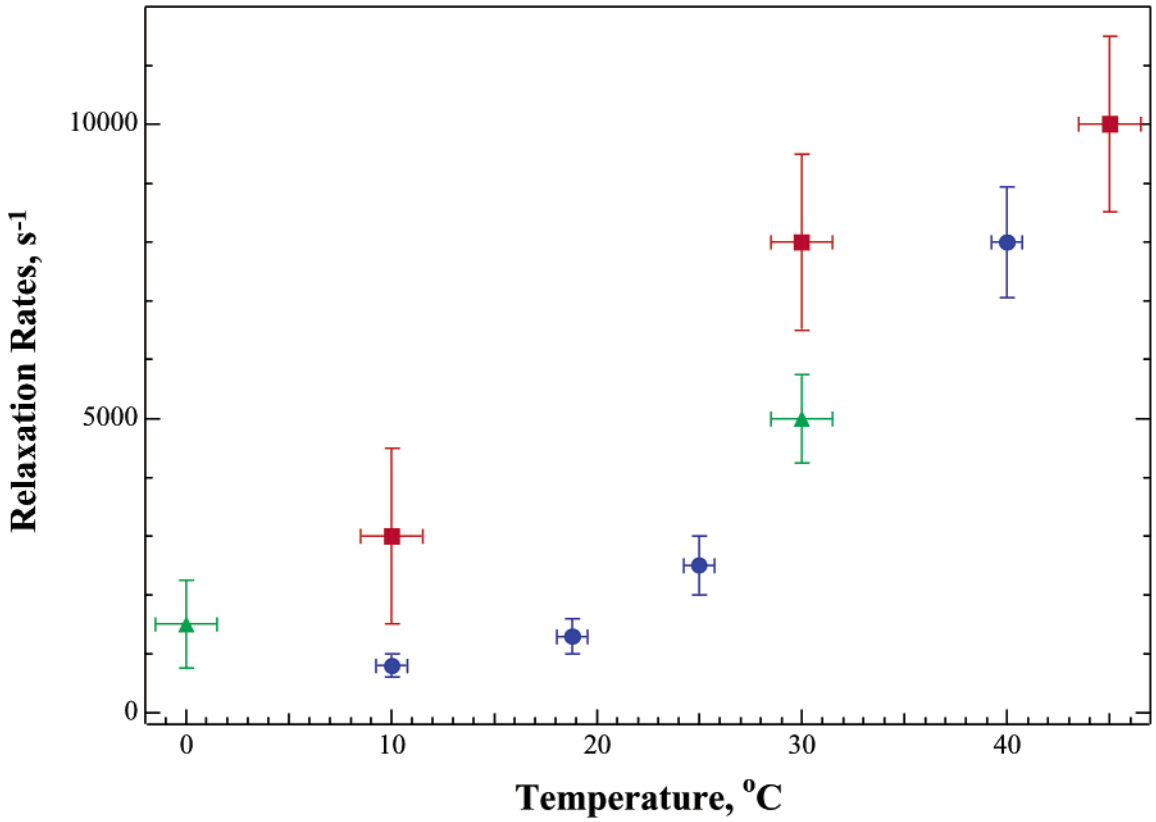

FIGURE 10: Rates of loop opening from NMR experiments are plotted together from those from this work. Measurements by solid state NMR are in red (*15*), those from solution state NMR are in green (*14*), and those from fluorescence (this paper) are in blue.

process we study is indeed the loop opening and ligand release.

Excellent agreement with prior experimental kinetic values for loop opening is afforded in these data. Figure 10 shows a compilation of rates measured for the loop opening on G3P under similar experimental conditions, by solid state and solution NMR (*14*, *15*) and by T-jump fluorescence methods (this paper). It is remarkable that two methods so different in experimental bias can achieve agreement in a kinetic phenomenon. Beyond this reassuring quantitative agreement, the NMR and fluorescence agree in other respects as well, most specifically that both methods show pronounced ligand dependencies. Furthermore, Knowles et al. have suggested that the rate of product release (of the order of 4000 s^{-1}), as measured by deuterium isotope effects, is related to the loop motion (*42*). It must be noted that the loop opening and ligand release steps are combined into a single pseudo-bimolecular constant in the prior enzymological analysis. Furthermore, the inability to decompose k_{on} and k_{off} separately prevents us from making a detailed comparative analysis. Nonetheless, all the data agree that a slow off rate is expected, of the order of 7000 s^{-1} for substrates at room temperature, and also that the apparent on rate is reduced much below the diffusion limit. The implication for the enzymological process is that the intermediate of the reaction is likely to be protected from solvent, as expected.

Several new thermodynamic facets are uncovered in this kinetic study. The division of enthalpy into two steps is made for the first time: the loop opening step to form the encounter complex formation is distinct from the ligand disassociation step. The major portion of the enthalpic value driving ion binding appears to be associated with ligand dissociation. Lacking structural data on an encounter complex, and a deeper and more precise thermodynamic analysis including heat capacity and entropy, we cannot fully rationalize the apparent temperature independence of the loop opening reaction in terms of structurally driven concepts. Certainly hydration, ion burial, and changes in hydrophobic exposed area are expected to occur in both steps to some extent. Nonetheless, our data show that loop opening reaction on the ligated complex has a 1:20 population of the open/closed ligated state with a fairly flat temperature dependence. The competency of the enzyme probably depends on both the rate constants for opening and the populations of open and closed states. For the intermediates of the reaction, coverage is essential, but for product release a moderate population of the encounter complex is needed. This balance appears to be preserved in a robust way over temperature.

Comparison of the behavior of the enzyme in the presence of G3P to that in the presence of PGA and phosphate unveiled some additional complexities of this system. Clearly, the rate and amplitude of the protein conformational change is dependent upon the ligand (Figure 4). In the presence of PGA the kinetic effect is masked, almost certainly because the kinetic phase is out of our time window on the slow side (relaxation times greater than 1 ms). The kinetic characteristics of loop opening in the relatively tight binding TIM−PGA complex were similarly difficult to observe by NMR. For the phosphate ligand, complex multiexponential behavior was observed, including phases much slower than those for G3P. While simple exponential decay laws are the Occum's razor for all of chemical and biochemical sciences, such a simplification is apparently valid for this enzymatic loop opening only when an ap-

propriately designed ligand is present. A distributed dynamical picture is needed to describe the kinetic behavior of the TIM−phosphate complex presumably because of the rather sloppy fit of the phosphate group in the active site (*43*−*47*). Therefore, in the presence of a simple phosphate ion, in the absence of any organic portion, the loop does not have a characteristic time scale but rather exhibits distributed dynamics in the opening reaction.

Our limited preliminary data on the enzyme−substrate complex and on enzyme−inhibitor complexes validate the notion that the G3P is an excellent mimic for the substrate and product. The simple and satisfying picture that emerges is that substrate release is kinetically limited by an activated loop opening. Furthermore, the loop can distinguish between various states along the reaction pathway and opens only at the beginning or end of the reaction but not in the intermediate. In other words, the character of the organic portion of the ligand−protein contacts may change through the reaction pathway and thereby may modulate the loop's opening rate. This is in agreement with the free energy profile as determined by Albery and Knowles: loop motion and hence ligand release may be partially rate limiting in the thermodynamically uphill reaction from DHAP to GAP. The chemical features that make it possible for the loop opening rate to be moderated are not clear based on this study, but one might speculate that the charges and ionization states of the ligand and nearby acids and bases are the most likely principles at work.

REFERENCES

1. Falzone, C. J., Wright, P. E., and Benkovic, S. J. (1994) *Biochemistry 33*, 439−442.
2. Wang, G. P., Cahill, S. M., Liu, X. H., Girvin, M. E., and Grubmeyer, C. (1999) *Biochemistry 38*, 284−295.
3. Waldman, A. D., Clarke, A. R., Wigley, D. B., Hart, K. W., Chia, W. N., Barstow, D., Atkinson, T., Munro, I., and Holbrook, J. J. (1987) *Biochim. Biophys. Acta 913*, 66−71.
4. Ito, Y., Yamasaki, K., Iwahara, J., Terada, T., Kamiya, A., Shirouzu, M., Muto, Y., Kawai, G., Yokoyama, S., Lane, E. D., Walchli, M., Shibata, T., Nishimura, S., and Miyazawa, T. (1997) *Biochemistry 36*, 9109−9119.
5. Johnson, L. N., and Wolfenden, R. (1970) *J. Mol. Biol. 47*, 93−100.
6. Albery, W. J., and Knowles, J. R. (1976) *Biochemistry 15*, 5627−5631.
7. Banner, D. W., Bloomer, A. C., Petsko, G. A., Phillips, D. C., Pogson, C. I., and Wilson, I. A. (1975) *Nature 255*, 609−614.
8. Alber, T., Banner, D. W., Bloomer, A. C., Petsko, G. A., Phillips, D., Rivers, P. S., and Wilson, I. A. (1981) *Philos. Trans. R. Soc. London, Ser. B 293*, 159−171.
9. Lolis, E., and Petsko, G. A. (1990) *Biochemistry 29*, 6619−6625.
10. Jogl, G., Rozovsky, S., McDermott, E. A., and Tong, L. (2003) *Proc. Natl. Acad. Sci. U.S.A. 100*, 50−55.
11. Pompliano, D. L., Peyman, A., and Knowles, J. R. (1990) *Biochemistry 29*, 3186−3194.
12. Sampson, N. S., and Knowles, J. R. (1992) *Biochemistry 31*, 8488−8494.
13. Sampson, N. S., and Knowles, J. R. (1992) *Biochemistry 31*, 8482−8487.
14. Rozovsky, S., and McDermott, A. E. (2001) *J. Mol. Biol. 310*, 259−270.
15. Rozovsky, S., Jogl, G., Tong, L., and McDermott, A. E. (2001) *J. Mol. Biol. 310*, 271−280.
16. Palmer, A. G. (2001) *Annu. Rev. Biophys. Biomol. Struct. 30*, 129−155.
17. Palmer, A. G., Williams, J., and McDermott, A. (1996) *J. Phys. Chem. 100*, 13293−13310.
18. Eftink, M. R. (1994) *Biophys. J. 66*, 482−501.
19. Bernasconi, C. F. (1976) *Relaxation Kinetics*, Academic Press, New York.
20. Putman, S. J., Coulson, A. F., Farley, I. R., Riddleston, B., and Knowles, J. R. (1972) *Biochem. J. 129*, 301−310.
21. Fersht, A. (1999) *Structure and Mechanism in Protein Science: A Guide to Enzyme Catalysis and Protein Folding*, Vol. 3, W. H. Freeman and Company, New York.
22. Williams, S., Causgrove, T. P., Gilmanshin, R., Fang, K. S., Callender, R. H., Woodruff, W. H., and Dyer, R. B. (1996) *Biochemistry 35*, 691−697.
23. Gulotta, M., Gilmanshin, R., Buscher, T. C., Callender, R. H., and Dryer, R. B. (2001) *Biochemistry 40*, 5137−5143.
24. Deng, H., Zhadin, N., and Callender, R. (2001) *Biochemistry 40*, 3767−3773.
25. Klein, R., Tatischeff, I., Bazin, M., Santus, R. (1981) *J. Phys. Chem. 85*, 670−677.
26. Harris, L. H., and Hudson, B. S. (1990) *Biochemistry 29*, 5276−5285.
27. Chen, Y., and Barkley, M. D. (1998) *Biochemistry 37*, 9976−9982.
28. Lambeir, A. M., Opperdoes, F. R., and Wierenga, R. K. (1987) *Eur. J. Biochem. 168*, 69−74.
29. Plaut, B., and Knowles, J. R. (1972) *Biochem. J. 129*, 311−320.
30. Campbell, I. D., Jones, R. B., Kiener, P. A., and Waley, S. G. (1979) *Biochem. J. 179*, 607−621.
31. Nickbarg, E. B., and Knowles, J. R. (1988) *Biochemistry 27*, 5939−5947.
32. Collins, K. D. (1974) *J. Biol. Chem. 249*, 136−142.
33. Amyes, T. L., O'Donoghue, A. C., and Richard, J. P. (2001) *J. Am. Chem. Soc. 2001*, 11325−11326.
34. Verlinde, C. L., Noble, M. E., Kalk, K. H., Groendijk, H., Wierenga, R. K., and Hol, W. G. (1991) *Eur. J. Biochem. 198*, 53−57.
35. Anfinrud, P. A., Han, C., and Hochstraser, R. M. (1989) *Proc. Natl. Acad. Sci. U.S.A. 86*, 8387−8391.
36. Richard, L., Genberg, L., Deak, J., Chiu, H.-L., and Miller, R. J. D. (1992) *Biochemistry 31*, 10703−10715.
37. Gulotta, M., Deng, H., Deng, H., Dyer, R. B., and Callender, R. H. (2002) *Biochemistry 41*, 3353−3363.
38. Williams, J. C., and McDermott, A. E. (1995) *Biochemistry 34*, 8309−8319.
39. Wierenga, R. K., Noble, M. E., Vriend, G., Nauche, S., and Hol, W. G. (1991) *J. Mol. Biol. 220*, 995−1015.
40. Cantor, C. R., and Schimmel, P. R. (1980) *Biophysical Chemistry*, Vol. 3, W. H. Freeman and Company, San Francisco.
41. Rigler, R., and Ehrenberg, M. (1973) *Quarterly Rev. Biophys. 6*, 139−199.
42. Maister, S. G., Pett, C. P., Albery, W. J., and Knowles, J. R. (1976) *Biochemistry 15*, 5607−5612.
43. James, D. R., and Ware, W. R. (1985) *Chem. Phys. Lett. 120*, 455−459.
44. Vix, A., and Lami, H. (1995) *Biophys. J. 68*, 1145−1151.
45. Kaplan, J. I., and Garroway, A. N. (1982) *J. Magn. Reson. 49*, 464−475.
46. Schaefer, D., and Spiess, H. W. (1992) *J. Chem. Phys. 97*, 7944−7954.
47. Basirov, A. B., Usmanov, S. M., and Zelenev, J. V. (1984) *Acta Polymerica 35*, 334−335.

BI026994I